공학석사 학위논문

Evaluation of Frequency-dependent Aerodynamic Admittance Function in a Time Domain Buffeting Analysis

시간영역 버페팅 해석을 위한 주파수 의존적인 공력 어드미턴스 함수의 산정법

2013 년 8월

서울대학교 대학원

건설환경공학부

김 상 원

ABSTRACT

A time-domain buffeting analysis considering aerodynamic admittance function is presented. The Fourier series approach (FSA) is adopted and extended to consider frequency-dependent aerodynamic admittance function and self-excited force. This adopted method is verified by comparing with a conventional method, the rational function approach (RFA). The admittance function of a bridge deck is extracted from experiments. The admittance function measured from the experiment showed difference with theoretical Sears' function for airfoil cross-sections. This measured aerodynamic admittance function is approximated successfully by FSA. The introduced scheme is applied to the full FEM model of a cable-stayed bridge. Comparison of the response from the Sears' function and experimentally extracted admittance function is dis cussed.

KEY WORDS:

Time-domain buffeting analysis, Aerodynamic admittance function, Fourier series approach

Student Number: 2011-23393

Table of Contents

List of Figures

List of Tables

Chapter 1

Introduction

From conventional aeronautics, the Sears function (Sears 1941) has been widely used as an aerodynamic admittance function for bridge deck in a relation to vertical wind component. The Sears function is derived theoretically from streamlined airfoil. That's why it may not be appropriate to apply the Sears' function to all types of sections. Scanlan and Jones (1999) and Hatanaka (2002) mentioned that an aerodynamic admittance function of a bluff section could be different from the Sears' function. For this reason, there were several attempts to evaluate an admittance function from the flutter derivatives. Unfortunately, this kind of indirect way to get an admittance function is not examined enough even if can circumvent difficulties of experiment to obtain admittance function. Therefore it is necessary to measure admittance function by an experiment before adopting the Sears' function as admittance function.

Furthermore to consider admittance function in a time-domain, the rational function approach (RFA) has been used and it is appropriate for smooth type admittance function (Caracoglia and Jones 2003). Measured admittance function, however, is not always in a smooth shape. For example the admittance function of Humber Bridge shows a wiggling shape (Diana et al. 2002). Since the basis function of RFA is rational function, it may not be the best way to use RFA for a

wiggling-shaped admittance function. In addition, several potential limitations of RFA are proposed by Caracoglia and Jones (2003) and Jung et al. (2012). To avoid these limitations of RFA, Park (2013) proposed a Fourier series approach (FSA) for the self-excited force. Aerodynamic transfer function corresponding to the deck motion can be approximated successfully with trigonometric functions and the causality condition is strongly imposed at the same time. Conception of this proposed method can be extended to evaluate admittance function.

Chapter 2

Fourier Series Approach for Aerodynamic Admittance Function

Lift, drag force and moment can be separated into three parts; force for average wind velocity, force induced by wind velocity fluctuation and motion-induced force (self-excited force). Wind direction and bridge axis is defined in Fig 2.1.

$$\begin{aligned} L &= L_{\text{average}} + L_{\text{buffet}} + L_{\text{self}} \\ D &= D_{\text{average}} + D_{\text{buffet}} + D_{\text{self}} \\ M &= M_{\text{average}} + M_{\text{buffet}} + M_{\text{self}} \end{aligned} \tag{2.1}$$

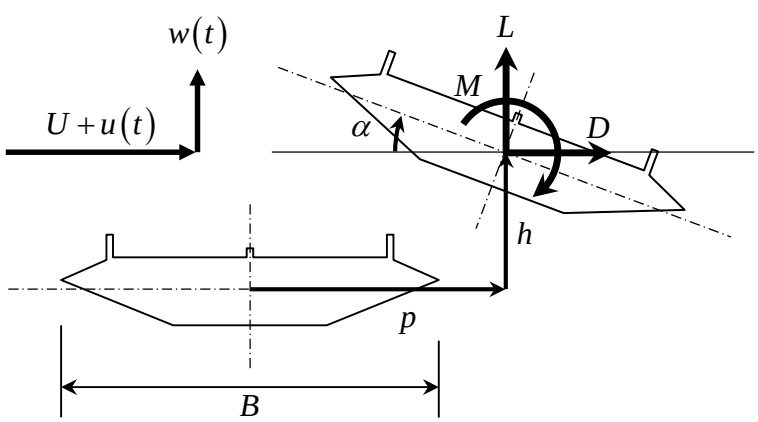

Fig 2.1. Bridge axis and wind component on the deck

For wind velocity fluctuation, the sectional buffeting forces (L_{buffet}, D_{buffet} and M_{buffet}) have conventionally been written in quasi-static terms (Strommen

2010):

$$L_b(x,t) = \frac{\rho U^2 B}{2}\left(2\chi_{Lu} C_L \frac{u}{U} + \chi_{Lw}\left(C_L' + C_D\right)\frac{w}{U}\right) \tag{2.2.a}$$

$$D_b(x,t) = \frac{\rho U^2 B}{2}\left(2\chi_{Du} C_D \frac{u}{U} + \chi_{Dw}\left(C_D' - C_L\right)\frac{w}{U}\right) \tag{2.2.b}$$

$$M_b(x,t) = \frac{\rho U^2 B^2}{2}\left(2\chi_{Mu} C_M \frac{u}{U} + \chi_{Mw} C_M' \frac{w}{U}\right) \tag{2.2.c}$$

where ρ = air density; U = mean wind velocity; u and w = longitudinal and vertical wind velocity fluctuation component; χ_{kl} = aerodynamic admittance function; and C_m and C_m' = static coefficients and its 1st derivative, relatively, for $i = L$, D and M. In this study, the second term of Eq. (2.2.a) is only demonstrated in detail.

Costa (2007) proposed one-sided convolution integral of aerodynamic forces induced by wind velocity fluctuation. Therefore lift force induced by w-direction wind component is expressed as follow:

$$L_{Lw}(t) = \frac{1}{2}\rho U^2 B\left(C_L' + C_D\right)\int_0^t \Phi_{Lw}\left(t-\tau\right)\frac{w(t)}{U}d\tau \tag{2.3}$$

where Φ_{Lw} = the Lw-component of aerodynamic impulse response function. Fourier transform of 2nd term of Eq. (2.2.a) and Eq. (2.3) should be same. In the end, aerodynamic admittance function should be same with transfer function

mathematically:

$$\frac{1}{2}\rho UB\left(C_L' + C_D\right)\chi_{Lw} w(\omega) = \frac{1}{2}\rho UB\left(C_L' + C_D\right)\phi_{Lw}(\omega)\bar{w}(\omega)$$
$$\chi_{Lw} = \phi_{Lw}(\omega) \tag{2.4}$$

where ϕ_{Lw} = the Lw-component of aerodynamic transfer response function. By Fourier series approach (FSA), this transfer function can be successfully approximated and causality of impulse response function is strongly imposed at the same time (Park 2013). Since transfer function is equivalent to aerodynamic admittance function, FSA can be applied to admittance function with the same manner.

$$\chi_{Lw} = \chi_{Lw}^R + i\chi_{Lw}^I \tag{2.5}$$

$$\bar{\chi}_{Lw}^R(K) = a_{Lw}^0 + \sum_{n=1}^{N} a_{Lw}^n \cos\frac{n\pi}{K_{\max}}K \tag{2.6.a}$$

$$\bar{\chi}_{Lw}^I(K) = b_{Lw}^0 K - \sum_{n=1}^{N} a_{Lw}^n \sin\frac{n\pi}{K_{\max}}K \tag{2.6.b}$$

where χ_{Lw}^R and χ_{Lw}^I = Real and Imaginary part of aerodynamic admittance function; $\bar{\chi}_{Lw}^R$ and $\bar{\chi}_{Lw}^I$ = Real and Imaginary part of approximated admittance function; and a_{Lw}^n and b_{Lw}^0 = unknown coefficients of the Fourier series; N = the number of terms in the Fourier series. Unknown coefficients are obtained by least square method (Park 2013). Impulse response function and lift force can be

expressed with FSA coefficients as follow:

$$\bar{\Phi}_{kl}\left(t\right)=a_{kl}^{0}\delta\left(t\right)+b_{kl}^{0}\frac{B}{U}\dot{\delta}\left(t\right)+\sum_{n=1}^{N}a_{kl}^{n}\delta\left(t-\frac{B}{U}\frac{n\pi}{K_{\max}}\right) \tag{2.7}$$

$$\begin{aligned}L_{Lw}\left(x,t\right)=\frac{1}{2}\rho U^{2}B\left(C_{L}'+\bar{C}_{D}\right)\Bigg(&a_{kl}^{0}\frac{w\left(t\right)}{U}+b_{kl}^{0}\frac{B}{U}\frac{\dot{w}\left(t\right)}{U}\\&+\sum_{n=1}^{N}\frac{a_{kl}^{n}}{U}w\left(t-\frac{B}{U}\frac{n\pi}{K_{\max}}\right)\Bigg)\end{aligned} \tag{2.8}$$

Chapter 3

Admittance Function Extraction Experiment

3.1. Devices and Test Setting

The active turbulence generator (Fig 3.1) consists of a series of wings linked together to produce vertical wind component. Motion of airfoil is driven by an electric motor. Amplitude and angular velocity of wing motion are determined by user. The bridge deck section selected for test is 1:36 scale model of 2nd Jindo Bridge. This Bridge has main span length of 344 m, which is located in between Haenam and Jindo, Korea.

Both-end-fixed test is carried out with three axes force measurement load cell. Hot wire anemometer measures wind velocity fluctuation which installed at upwind of the bridge model with far enough distance to avoid disturbance (Fig 3.2). All tests are conducted at the wind tunnel laboratory of Seoul National University in Seoul, Korea.

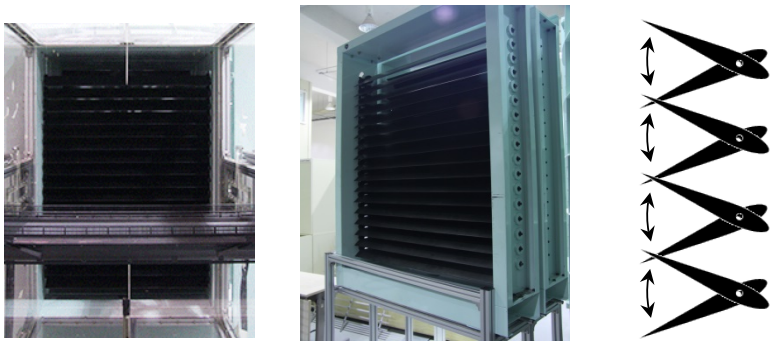

Fig 3.1. Active turbulence generator

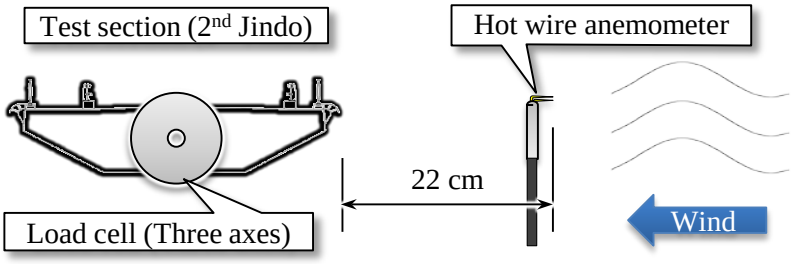

(a)

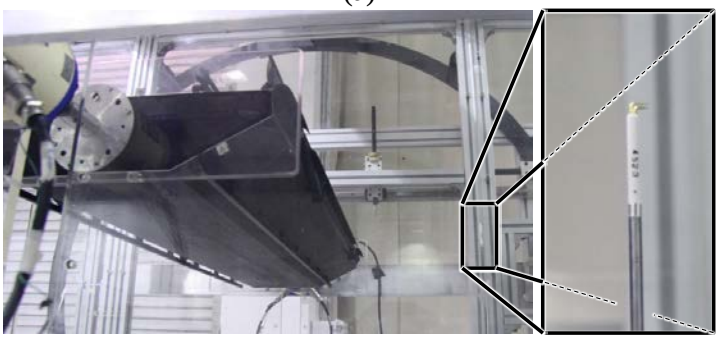

(b)

Fig 3.2. Setting of admittance function Extraction Experiment: (a) mimetic diagram of the test setting; and (b) Actual setting at the wind tunnel

3.2. Post Process of Raw Data

From Eq. 2.2.a, lift force induced by vertical wind component is:

$$L_b\left(x,t\right)=\frac{\rho U^2 B}{2}\chi_{Lw}\left(C_L'+C_D\right)\frac{w}{U} \tag{3.1}$$

Assume vertical wind velocity component is sinusoidal wave; $w\left(t\right)=w_0\sin\left(\omega_w t\right)$. Then lift force will also be harmonic force with phase lag, θ_{Lw}. Therefore Eq. (3.1) can be expressed as follow:

$$L_{w0}\sin\left(\omega_w t+\theta_{Lw}\right)=\frac{\rho UB}{2}\chi_{Lw}\left(C_L'+C_D\right)w_0\sin\left(\omega_w t\right) \tag{3.2}$$

By taking Fourier transform, the admittance function can be determined with amplitude of lift and vertical wind velocity component and phase lag:

$$\left(\chi_{Lw}^R+i\chi_{Lw}^I\right)=\frac{2L_{w0}}{w_0\rho UB\left(C_L'+C_D\right)}\left(\cos\left(\theta_{Lw}\right)+i\sin\left(\theta_{Lw}\right)\right) \tag{3.3}$$

$$\chi_{Lw}^R=\frac{2L_{w0}\cos\left(\theta_{Lw}\right)}{w_0\rho UB\left(C_L'+C_D\right)},\quad \chi_{Lw}^I=\frac{2L_{w0}\sin\left(\theta_{Lw}\right)}{w_0\rho UB\left(C_L'+C_D\right)} \tag{3.4}$$

where w_0, ω_w = circular frequency and amplitude of vertical wind velocity component, respectively; L_{w0}, θ_{Lw} = amplitude and phase lag of lift force, respectively. If ω_w, L_{w0} and θ_{Lw} could be measured, real and imaginary part of

admittance function are determined.

Unfortunately, measured wind velocity fluctuation and lift force is not neat sinusoidal signal even if the motion of the airfoil is utmost harmonic. Because of unpredictable and mechanical noise, high-frequency components are mixed with raw data. It is the reason why a filter is necessary which adopts dominant frequency component. With sinusoidal function, $A\sin\left(Bt+C\right)$, raw data can be smoothed into clean harmonic signal. Least square method can determine all unknown variable of sine function. Then amplitude and phase of each data also are determined. Raw data and smoothed signal is presented in Fig 3.3.

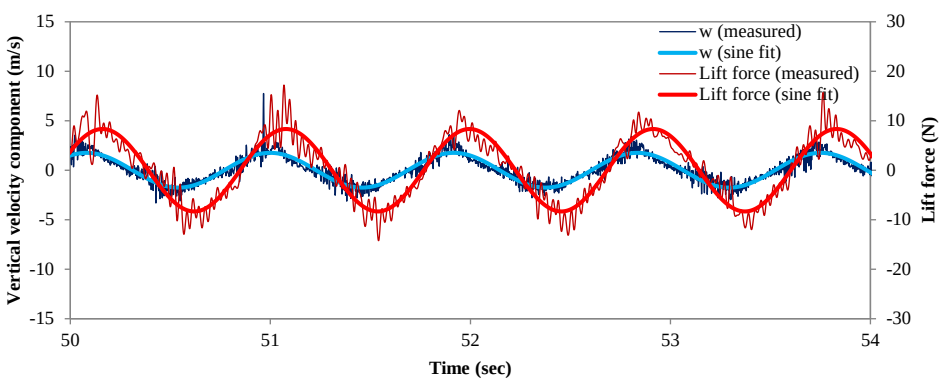

Fig 3.3. Raw and smoothed data measured from the test

To guarantee consistency of the test experiment is carried out with two different frequency of airfoil wing. Total 4 trials are conducted to get admittance function. If both width of the bridge deck model and angular frequency of airfoil motion are fixed, reduced frequency is controlled by average wind velocity. The

experiment, hence, is performed with fixed angular frequency and various wind velocity to cover wide range of reduced frequency. Same procedure is repeated twice in 1.0 Hz and 1.5 Hz, respectively. The result is regressed with 6-order polynomial (Fig 3.4). As shown in Fig 3.5, measured admittance function of 2nd Jindo Bridge deck is somewhat different from Sears' function. This measured admittance function has a wiggling-shaped profile.

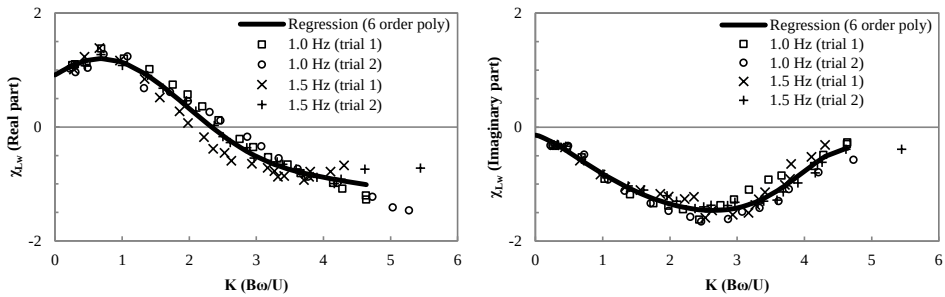

(a) (b)

Fig 3.4. Measured admittance function and its regression: (a) real component of measured admittance function; and (b) imaginary component of measured admittance function

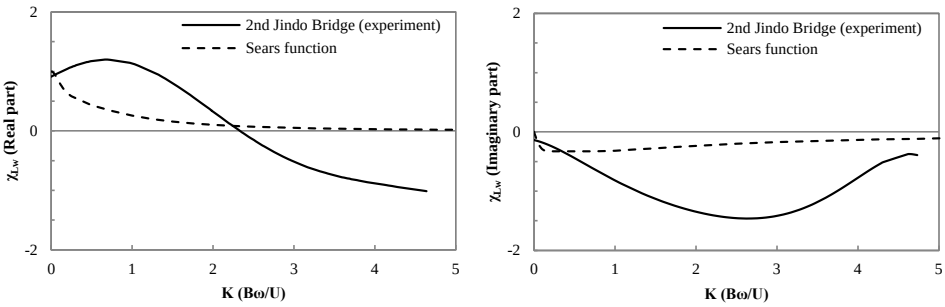

(a) (b)

Fig 3.5. Comparison of Sears' function and measured admittance function: (a) real component of admittance function; and (b) imaginary component of admittance function

Chapter 4

FSA Applications and Buffeting Analysis

4.1. Rectangular section of B/D=20

To verify validity of FSA on the admittance function, RFA can be a reference method to compare. Sears' function is adopted as an aerodynamic admittance function. Sears' function used in this analysis is approximated one by Jones (1940) with couple of indicial functions. Since Fourier transform of indicial function is rational function in frequency domain, RFA can yield exact solution for Sears' function. On the other hand, it needs a number of trigonometric functions to make good fitness by FSA, because Sears' function is in smooth shape and FSA is good for wiggling shaped admittance function. Results of FSA coefficient optimization is shown in the Fig 4.1. Total 75 trigonometric functions are used to obtain good fitness. Static coefficients and its first order derivatives used in analysis is summarized Table 4.1.

The wind velocity fluctuation is generated by ARMA (Auto-regression moving average) technique. Spectrum of wind velocity fluctuation is Von Karman spectrum (Von Karman 1948). A turbulence intensity of 20% is adopted for horizontal direction and half of this for vertical direction. A length scale of 1.25 m is selected for horizontal direction and 1/8 of this for vertical direction. Mean wind velocity is equal to 4 m/s and an air density of 1.25 kg/m^3 is used. Analysis

period is 100 seconds and time interval, Δt is equal to 0.05 sec. Newmark's beta method with β = 1/6, γ = 1/2 is adopted for the time integration. Mechanical properties of the structural system are shown in the Table 4.2.

Self-excited forces for the section are considered by FSA as well. Flutter derivatives are extracted at the laboratory of Seoul National University in Seoul, Korea.

Analyzed responses are shown in the Fig 4.2. Both RFA and FSA cases reduce the response down from Unity admittance case. Negligible differences are observed in the vertical response between the results of RFA and FSA.

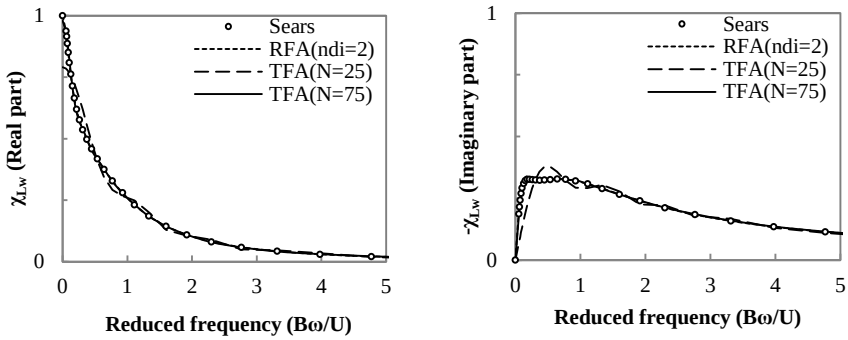

(a) (b)

Fig 4.1. Result of TFA and RFA coefficient optimization: (a) real component of admittance function; and (b) imaginary component of admittance function

Table 4.1. The static coefficients and its first-order derivatives

Type of section	C_L	C_D	C_M	$\left.\frac{\partial C_L}{\partial \vartheta}\right\|_{\vartheta=0}$	$\left.\frac{\partial C_D}{\partial \vartheta}\right\|_{\vartheta=0}$	$\left.\frac{\partial C_M}{\partial \vartheta}\right\|_{\vartheta=0}$
B/D 20	-	-	-	-7.65	-	-0.77
2nd Jindo Bridge	0.022	0.197	0.047	0.182	1.997	0.489

Table 4.2. Mechanical properties of the structural system

Mass	m_k $(\mathrm{kg/m})$	4.964
	m_a $(\mathrm{kg \cdot m^2/m})$	0.140
Damping ratio	ξ_k (%)	0.274
	ξ_a (%)	0.129
Frequency	f_k (Hz)	2.272
	f_a (Hz)	3.977

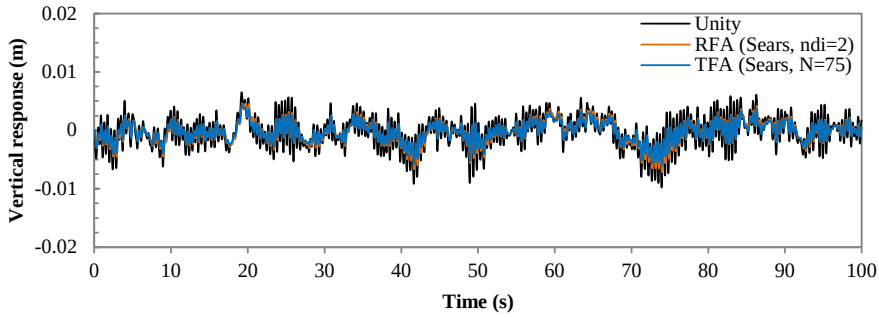

(a)

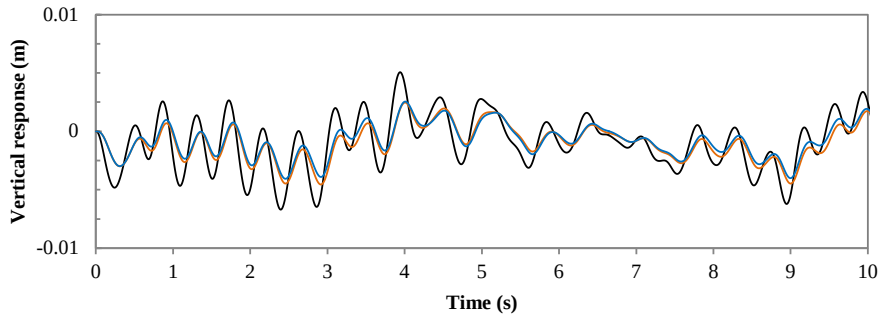

(b)

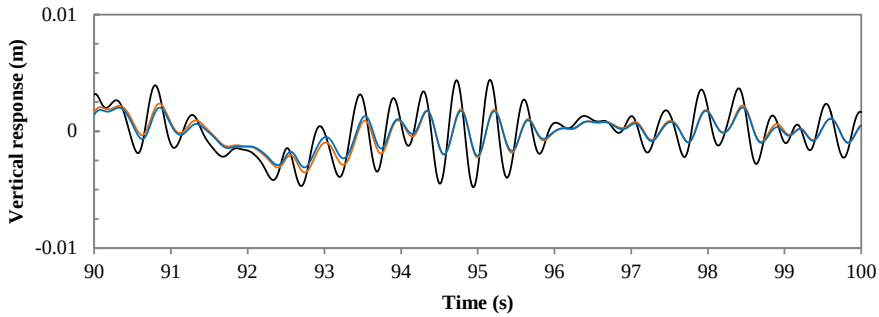

(c)

Fig 4.2. Buffeting responses by RFA and FSA of B/D 20 section model with Sears' function: (a) vertical response at a wind velocity of 4 m/s for 100 sec; (b) vertical displacement for t = 0~10 sec; (c) vertical displacement for t = 90~100 sec

4.2. Large-scale Bridge: 2nd Jindo Bridge

The aerodynamic admittance function measured in Chapter 3 can be approximated with trigonometric function via least square method. After this optimization, all FSA coefficients will be obtained. Truncated order of Fourier series, N, is equal to 20. Higher truncated order than 20 doesn't work to get finer fit. And for the sake of brief calculation, the less truncated order is the better. Therefore truncated order of 20 is effective for analysis. Self-excited forces for the buffeting analysis are considered by FSA as well. Flutter derivatives of 2nd Jindo Bridge are extracted at the laboratory of Seoul National University in Seoul, Korea.

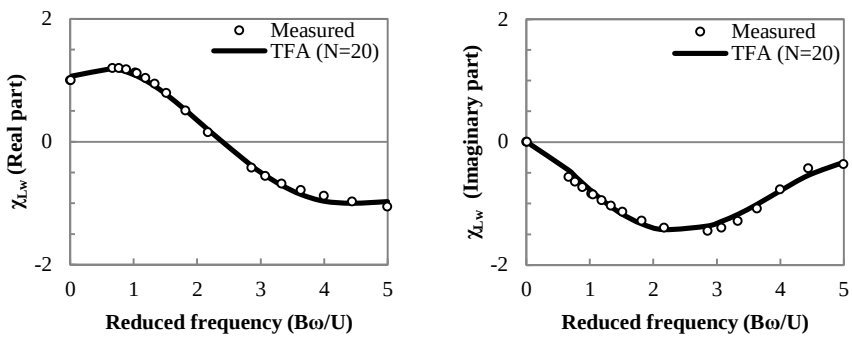

(a) (b)

Fig 4.3. Result of TFA coefficient optimization: (a) real component of admittance function; and (b) imaginary component of admittance function

3-dimensional FEM frame element and equivalent stiffness truss element are used for frame element and cable element, respectively. Analysis model is drawn in Fig 4.4. Rayleigh damping is used for structural damping and 0.4% is chosen for

the modal damping ratio as written in KSCE (2006). Total thirty modes are chosen from the lowest mode for buffeting analysis. Since the effect of self-excited force can be ignored, the effect of aerodynamic damping and stiffness is not considered in modal analysis.

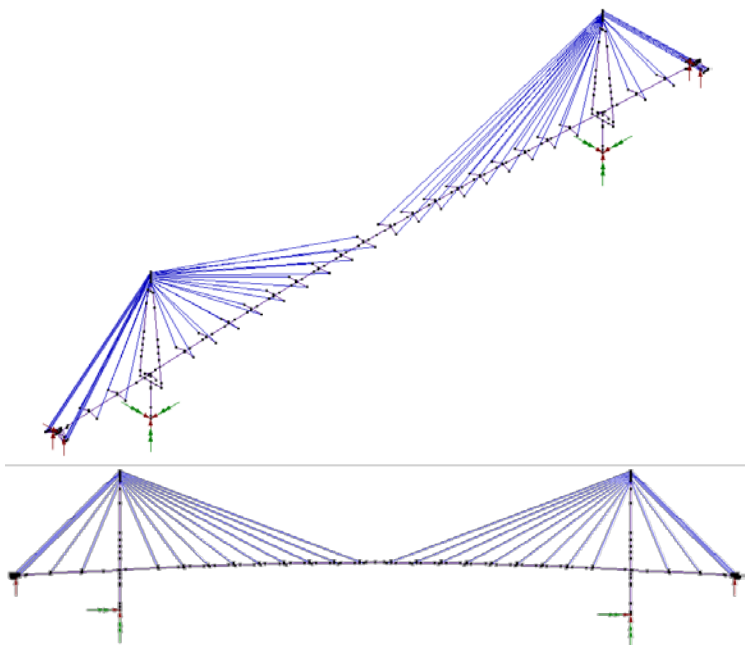

Fig 4.4. 3-D analysis model of 2nd Jindo Bridge

The lift force of deck section is calculated as Eq. (2.8). Assume that the sectional force is homogeneous along the element axis and equivalent nodal force at the element ends is equal to the sum of sectional force corresponding to the half cord of the element. Wind velocity applied on element is assumed to be equal to mean velocity of both ends. Then the lift force induced by vertical wind component

can be expressed as follow:

$$L_w^i(t) = L_w^j(t) = \left(\frac{L}{2}\right) \cdot \frac{1}{2}\rho UB\left(C_L' + \bar{C}_D\right)\begin{pmatrix} a_{Dw}^0 w(t) + b_{Dw}^0 \frac{B}{U}\dot{w}(t) \\ + \sum_{n=1}^{N} a_{Dw}^n w\left(t - \frac{B}{U}\frac{n\pi}{K_{\max}}\right) \end{pmatrix} \quad (4.1)$$

where super-script i and j mean i-node and j-node of element, respectively and L = element length. The lift force is applied only on the main and side span but pylon and cable element. Static coefficients and its first order derivatives used in analysis is summarized Table 4.1.

The wind velocity fluctuation is generated by ARMA (Auto-regression moving average) technique. Spectrum of wind velocity fluctuation is Von Karman spectrum (Von Karman 1948). Turbulence intensity and Length scale is calculated as specified in KSCE (2006) and Stommen (2010), respectively and coherence is determined as proposed Iwatani (1982). Calculated values are summarized in Table 4.3. Generated wind velocity fluctuation is shown in Fig 4.5. Mean wind velocity is equal to 30 m/s and an air density of 1.25 $\mathrm{kg/m^3}$ is used. Analysis period is 600 seconds (10 minutes) and time interval, Δt is equal to 0.05 sec. Newmark's beta method with β = 1/6, γ = 1/2 is adopted for the time integration.

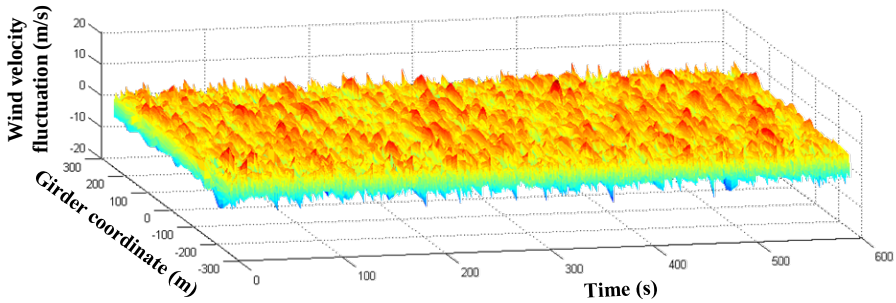

Fig 4.5. Generated vertical wind velocity fluctuation

Sears' function is adopted as a reference aerodynamic admittance function. Buffeting analysis is performed with Sears' function and measured admittance function. Sears' function decrease response down by 56% from unity admittance case. On the other hand, measured admittance function amplifies response 33% (Table 4.4). Time-domain response is shown in the Fig 4.6.

Table 4.3. Wind condition adopted for buffeting analysis

Spectrum (Von Karman 1948)	Horizontal: $\dfrac{f \cdot S_u(f)}{\sigma_u^2} = \dfrac{4 \cdot \hat{f}_u}{\left(1 + 70.8 \cdot \hat{f}_u^2\right)^{5/6}}$ Vertical: $\dfrac{f \cdot S_n(f)}{\sigma_n^2} = \dfrac{4 \cdot \hat{f}_u \left(1 + 755.2 \cdot \hat{f}_u^2\right)}{\left(1 + 283.2 \cdot \hat{f}_u^2\right)^{11/6}},\ n = v, w$
Turbulence intensity (KSCE 2006)	Horizontal: $I_u = \left(1/\ln\left(30/z_0\right)\right)\left(30/\max\left(z, z_b\right)\right)^{\alpha_I} = 12.8\ \%$ Vertical: $I_w = 0.5 I_u$
Length scale (Strommen 2010)	Horizontal: $L_u = L_0 \cdot \left(z/z_{b1}\right)^{\alpha_L} = 131.242\ m$ Vertical: $L_w = L_u/12$
Coherence (Iwatani 1982)	$\sqrt{Coh\left(z_1, z_2; n\right)} = \exp\left(-k_\eta n \eta / U\right)$ where $k_\eta = 14\left(\eta/z\right)^{0.45}$

Table 4.4. RMS and MAX value of buffeting response

Admittance	RMS (m)	MAX (m)
Unity	0.189	0.488
Sears' Function	0.083 (56 % decrease)	0.650 (57 % decrease)
Measured	0.251 (33 % increase)	0.210 (33 % increase)

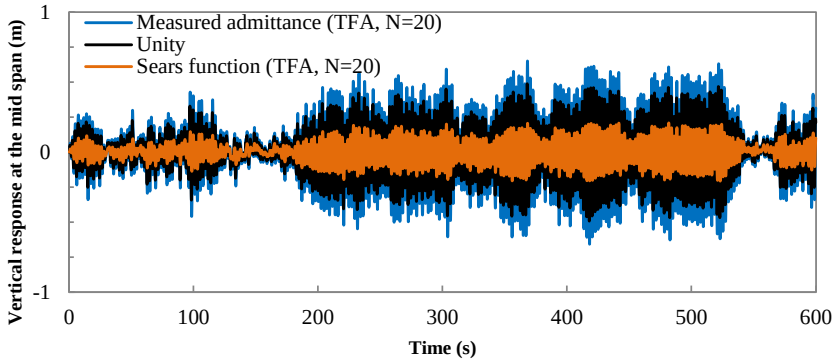

(a)

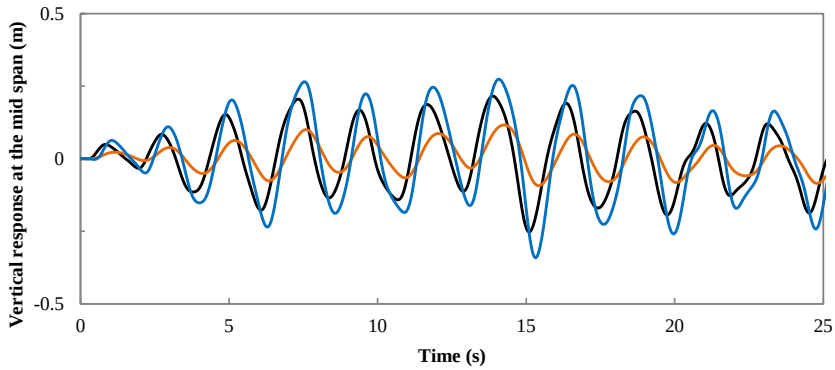

(b)

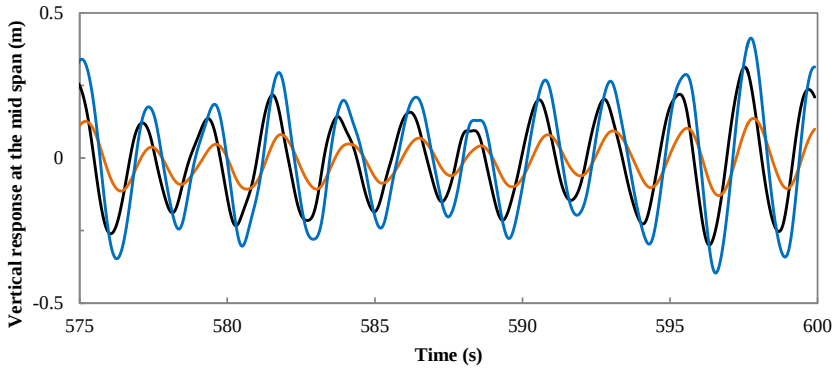

(c)

Fig 4.6. Buffeting responses of 2nd Jindo Bridge with 3 different admittance cases: (a) vertical response at a wind velocity of 30 m/s for the 2nd Jindo Bridge; (b) vertical displacement for t = 0~25 sec; (c) vertical displacement for t = 575~600 sec

Chapter 5

Summary and Conclusions

A new method using trigonometric function to consider frequency-dependent buffeting force is proposed. With this method, phase lag and amplitude change was successfully considered in a time-domain which comes from effect of an admittance function induced by wind velocity fluctuation. In addition, FSA strongly enforces the causality condition in the impulse response function required to perform one-sided convolution integral for a time-domain analysis. The FSA coefficients are determined through the optimization to minimize the error between the measured admittance function and the Fourier series. This method can be a solution to resolve several limitation of RFA on a bluff section.

The applicability of FSA is demonstrated through the examples on a box girder section and a real bridge. For box girder section, the time-domain analysis is performed with elastically supported system. Since the difference between the results from RFA and FSA is negligible, validity of FSA on aerodynamic admittance function is verified.

For the real bridge, 2nd Jindo Bridge, the time-domain buffeting analysis is performed with 30 modes and simulated wind velocity fluctuation. Three different aerodynamic admittance functions are adopted to analyze the structure: unity; Sears' function; measured admittance function. Generally, the Sears' function reduces

down the response from one of the unity case. Measured admittance function, however, can amplify the response bigger than one of unity case. In conclusion, admittance function should be adopted carefully.

REFERENCES

Sears, W. R. (1941) “Some aspects of non-stationary airfoil theory and its practical application.” J. Aeronautics Sci, 8(3), 104-108.

Scanlan, R. H. and Jones, N. P. (1999) “A form of aerodynamic admittance for use in bridge aeroelastic analysis,” J. Fluids and Struc. 13, 1017-1027.

Hatanaka, A. and Tanaka, H. (2002) “New estimation method of aerodynamic admittance function,” J. Wind Eng. Ind. Aerodyn. 90, 2073-2086.

Caracoglia, L., and Jones, N. P. (2003) “Time domain vs. frequency domain characterization of aeroelastic forces for bridge deck section,” J. Wind Eng. Ind. Aerodyn., 91, 371-402.

Diana, G., Bruni, S., Cigada, A. and Zappa, E. (2002) “Complex aerodynamic admittance function role in buffeting response of a bridge deck,” J. Wind Eng. Ind. Aerodyn., 90 2057-2072

Jung, K., Kim, H. K. and Lee H. S. (2012) “Evaluation of impulse response functions for convolution integrals of aerodynamic forces by optimization with a penalty function,” J. Eng. Mech., 138(5), 519-529.

Park, J. W. (2013) “Time-domain aeroelastic analysis of bridge using a truncated Fourier series of the aerodynamic transfer function,” Master dissertation, Seoul National University.

Strommen, E. N. (2010) Theory of Bridge Aerodynamics, Springer, pp.91-108.

Costa, C. and Borri, C. (2007) “Aerodynamic admittance function and buffeting forces for bridge via indicial functions”, J. Fluids and Struc., 23, 413-428.

Jones, R. T. (1940) “The unsteady lift on a wing of finite aspect ratio.” NACA Report 681, U.S. Nat. Advisory Committee for Aeronautics, Langley, Va

Von Karman, T. (1948) “Progress in the statistical theory of turbulence”, J. Maritime Research, Vol. 7.

KSCE (2006) Design guideline for steel cable-supported bridges.

Iwatani, Y. (1982) “Simulation of multidimensional wind fluctuations having any arbitrary power spectra and cross spectra”

초 록

이 연구는 공력 어드미턴스 함수를 고려한 시간영역 버페팅 해석방법을 제시한다. 주파수 의존적인 공력 어드미턴스 함수와 플러터 계수를 시간영역에서 고려하기 위해서 푸리에 급수를 이용하였다. 유리 함수를 이용한 접근 방법을 기준으로 하여, 푸리에 급수를 이용한 방법의 타당성을 검증한다. 실제 교량단면을 이용하여 공력 어드미턴스 함수가 실험을 통해서 추출된다. 이 측정된 공력 어드미턴스 함수는 유선형의 에어포일 단면으로부터 이론적으로 유도된 Sears 함수와는 다른 양상을 보인다. 푸리에 급수 전개를 이용하면 측정한 공력 어드미턴스 함수를 성공적으로 근사할 수 있다.

제시된 방법을 유한요소 전교 모형에 적용하여 버페팅 해석을 수행하고, Sears 함수와 측정된 공력 어드미턴스 함수를 각각 적용하여 응답을 구한다. 서로 다른 어드미턴스 함수를 적용하여 얻은 응답에 차이에 대해서 논의한다.

주요어:

시간영역 버페팅 해석, 공력 어드미턴스, 푸리에 급수를 이용한 접근 (Fourier series approach)

학번: 2011-23393